Processing and Application of Ceramics 18 [3] (2024) 235–243
https://doi.org/10.2298/PAC2403235X

Influence of starting WC particle size and sintering conditions on structure and properties of WC-Ni-Co coarse grain ceramics

Shubo Xu[1,*], Shengliang Wang[1], Chen Xu[2], Chenhao Zhao[1], Weihai Zhang[3], Wenming Wang[4], Liang Chen[3], Qihua Ren[4], Yuefei Pan[1], Jianing Li[1], Guocheng Ren[1], Fei Ni[1], Juanjuan Han[1]

[1]*Shandong Jianzhu University, School of Materials Science and Engineering, Jinan, 250101, China*
[2]*University of Nottingham, School of Computer Science, Nottingham, 250101, China*
[3]*Weifang Fuyuan Supercharger Co. LTD, Weifang, 261206, Shandong, China*
[4]*Shandong Wenling Precision Forging Technology Co. LTD, Jinan, 271100, Shandong, China*

Received 7 April 2024; Received in revised form 27 May 2024; Received in revised form 24 June 2024; Accepted 28 July 2024

Abstract

Sintering temperature is the key factor affecting the structure and performance of tungsten carbide (WC) ceramics. Thus, the effect of sintering temperature on the microstructure and mechanical properties of WC-Ni-Co coarse grain ceramics, obtained from the mixture containing: 60 wt.% of ultra-coarse WC, 30 wt.% of fine WC, 7 wt.% of Co and 3 wt.% of Ni powders, was analysed. The mechanical properties of WC ceramics did not change much when the sintering temperature was varied between 1410 and 1430 °C and the comprehensive performances of the ceramics were the best in this temperature range. In order to confirm that the coarse grain WC-Ni-Co ceramics can be applicable for harsh environments, it was compared with the standard WC-Co ceramics of the same grain size, and the reasons and mechanisms for the differences in microstructure and properties between the two ceramics were tested and analysed. The study shows that the average grain size of two ceramics does not differ much, and there are no decarburisation, graphite-phase and other impurity phases inside the ceramics. In addition, the difference in the mechanical properties is also small. However, the addition of Ni effectively improves the corrosion resistance of the WC-Co ceramics. Therefore, WC-Ni-Co can replace WC-Co ceramics as shield cutting tool material with the same grain size.

Keywords: *WC-Ni-Co ceramics, grain coarsening, microstructure, mechanical properties, wear resistance*

I. Introduction

Cemented carbide is a composite material consisting of tungsten carbide, the hard phase and cobalt, the binder phase metal [1]. It possesses high hardness, strength, toughness, wear resistance and corrosion resistance [2,3] and because of that often used for fabrication of metal cutting tools and wear-resistant parts [4,5]. Pure tungsten carbide was first synthesized in 1897 by Henri Moissan from W/C mixture by high-temperature sintering and it had high hardness [2,6]. However, its brittle and low toughness characteristics limited the wide range of application until Karl Schröter found that tungsten carbide (WC) with the addition of some metals has a certain toughness and resistance to tensile stress [6,7]. With the subsequent development of the metallurgical industry, WC ceramic products have been widely covered in metal cutting field, tunnelling, mining tools, oil drilling and construction and other industries [1,8]. In the past two decades, with the increase in the application of ceramics and the construction in the more demanding environment, the cemented carbides also put forward more and more high performance requirements.

Nowadays, most of the shield tool materials use ceramics with Co bonded to metal, which will lead to a large consumption of Co resources [9]. The world's cobalt resource reserves are low, and Co should be used sparingly as a strategic material. Thus, replacement of

*Corresponding author: tel: +86 15153166968
e-mail: *xsb@sdjzu.edu.cn*

Co has to be found and Ni can be used as the bonding metal to a certain extent. Research shows that the hardness and strength of Ni itself is lower than that of Co, and the solubility of Ni in tungsten carbide (WC) is higher than that of Co under high-temperature sintering [10]. The addition of Ni is prone to coarsening of grains, which leads to a significant reduction in the wear resistance of the cemented carbide. Therefore, it is of great research significance to study the inhibition of WC grain coarsening and improve the wear resistance of WC-Ni-Co ceramics.

Powder sintering is mainly a high temperature treatment process in which the powder compacts are heated to undergo mutual flow, melting and recrystallization reactions to achieve densification to improve strength and other properties [11]. Vacuum sintering [12] and low pressure sintering [13] are currently the most widely used methods for producing metal ceramics. Vacuum sintering can improve the wettability of Co binder on WC hard particles, accelerate the volatilisation of organics and oxides and the contraction process of the sintered body, and effectively improve the strength of ceramics. However, the liquid phase of vacuum sintered metal ceramics flows slowly, tiny pores still exist inside the ceramics, which cannot ensure the complete elimination of gases, and the lower densification leads to the reduced performance of the ceramics. The process of vacuum sintering after extracting the air, filling a certain amount of inert gas into the furnace and applying pressure to the powder compacts is known as low-pressure sintering [12,13]. Low-pressure sintering can promote the mobility of the liquid phase by applying pressure, fill the pores inside the ceramics to increase densification, and effectively improve the mechanical properties of ceramics.

During liquid-phase sintering, solid-phase particles are dissolved in the liquid phase and their average grain size grows through Ostwald ripening, a phenomenon in which large particles grow and small particles disappear. This phenomenon has been analysed theoretically by Lifshitz, Slyozov and Wagner and is known as the LSW theory [14,15]. The theory proposes two mechanisms of grain growth, diffusion-controlled and interfacial reaction-controlled in the kinetics of grain coarsening.

Sintering temperature is the key factor affecting the performance of ceramics and WC grain size during the sintering process [11,16] and is influenced by adding of Co as the binder phase. Nickel can also be added to improve the corrosion resistance, but in the same time it might reduce hardness, wear resistance and strength compared to WC-Co alloys [17,18].

II. Experimental

2.1. Sample preparation

Two WC powders with different particle sizes (one with ultra-coarse and another with fine WC particles) and Ni and Co powders, added as binder metals, were purchased from Jinan Metallurgical Scientific Research Co used for sample preparation. The mass fractions of the powders were the following: 60 wt.% of the powder with ultra-coarse WC particles, 30 wt.% of the powder with fine WC particles, 7 wt.% of Co powder and 3 wt.% of Ni powder.

The total amount of 500 g of the ingredients was poured into the ball mill jar together with 23% ethanol used as the dispersing medium. Wet grinding was carried out in the GQM-4-5 drum ball mill for 16 h at a speed of 60 rpm and the obtained wet milled mixture was dried in a vacuum drying oven. After that 2% paraffin wax, dissolved in gasoline, was added into the mixed powder, which was then again dried and sieved through a copper mesh (40-mesh and 80-mesh). Finally, the obtained ceramic powder mixture was pressed by a 30 T uniaxial hydraulic press at 15 kN pressure. The pressed samples were sintered in a German PVA low pressure sintering furnace at temperatures of 1390, 1410, 1430 and 1450 °C and argon pressure of 5 MPa. The sintered samples were labelled as A1, A2, A3 and A4, respectively (Table 1).

For comparison, two more control specimens were prepared by using only the ultra-coarse WC powder: i) WC-Ni-Co with 7 wt.% Co and 3 wt.% of Ni and ii) WC-Co with 10 wt.% Co. These sintered samples were labelled as D1 and D2, respectively (Table 1).

2.2. Sample characterization

The metallographic test specimens were prepared according to the Chinese national standard (GB/T3488.1-2014). The specimens were roughly ground by sandpaper, polished to roughness ≤1 μm and then corroded using metallographic corrosion solution (NaOH : $K_3[Fe(CN)_6]$ = 1 : 1) for 80–90 s. After that the specimens were cleaned with water and anhydrous ethanol and their surfaces were dried by a hair dryer. The sur-

Table 1. Composition and sintering condition of prepared samples

Sample	Ultra-coarse grain WC [wt.%]	Fine grain WC [wt.%]	Co [wt.%]	Ni [wt.%]	Sintering temperature [°C]
A1	60	30	7	3	1390
A2	60	30	7	3	1410
A3	60	30	7	3	1430
A4	60	30	7	3	1450
D1	90		7	3	1430
D2	90		10		1430

face of the cemented carbide was finally observed by the Leica DMI3000M metallographic microscope. In addition, the polished, fractured, wear-treated and corroded specimen surfaces were analysed by scanning electron microscope (SEM, PHENOM PW-100-018). Elemental composition was determined by using an energy spectrometer (EDS).

Hardness of the sintered sample was measured by Rockwell Hardness Tester (WH2002T) and Multifunctional Automatic Turret Digital Vickers Hardness Tester (MHVD-50AP). Bending strength and fracture toughness of the sintered specimens were measured by electronic universal testing machine (Jinan Kanghua PWS-100/V3.0) and Microcomputer-controlled electronic universal testing machine (Jinan Test King WDW-100L).

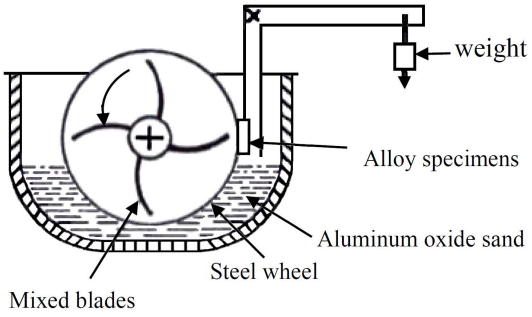

Figure 1. Experimental principle of the steel wheel method

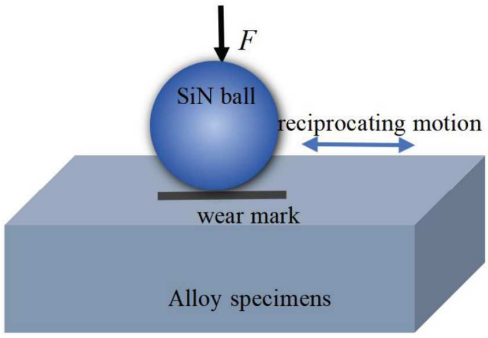

Figure 2. Test schematic diagram of carbide reciprocating friction wear experiment

The steel wheel method (Fig. 1) and reciprocating friction wear method were used to test the wear resistance of the WC-Ni-Co and WC-Co ceramics. Reciprocating friction experiments were carried out using the American Rtec MFT-5000 friction and wear tester for friction resistance experimental testing of ceramics, as shown in Fig. 2. Under room temperature conditions, the experiment was carried out by dry friction in the form of contact between the reciprocating ball and the test block. The wear parts were SiN balls with a diameter of 3 mm, and the test piece was a ceramics block prepared by a low-pressure sintering furnace. Prior to the friction and wear experiments, the ceramics was subjected to rough grinding by a grinder, fine grinding by a polishing machine and surface polishing to ensure that the roughness of the ceramics test surface was lower than 1 μm. The applied load in the experiments was 50 N, the sliding frequency was 8 Hz, the travelling length was 5 mm and the test time for each specimen was 30 min. At the end of the experiments, the friction resistance curve could be obtained directly from the wear tester by using a Sartorius-BSA126, which was used to test the wear test surface of the test piece. Sartorius-BSA124S precision balance was used to weigh the carbide specimens to calculate the mass loss.

III. Results and discussion

3.1. Effect of sintering temperature

The SEM micrographs of the ceramics sintered at different temperatures are shown in Fig. 3. The dark area indicates the Co-Ni bonding phase between the WC grains. Figure 4 illustrates the average grain size and adjacency for A1-A4 ceramics. Adjacency is defined as the ratio of the surface of WC grain boundary to the total surface of the boundary in the alloy and was used to indicate the degree of compactness of WC grains [19]. No obvious pores were found in the microstructure of the specimens sintered at temperatures between 1390–1450 °C, which indicates that the ceramics have high densities. Except for a slight difference in the average size of WC grains, the differences in the microstructures of the specimens at different sintering temperatures were very small. The average WC grain size increased slowly when the sintering temperature rose from 1410 to 1430 °C. However, when the sintering temperature increased to 1450 °C, the average WC grain size increased to 4.46 μm, which is due to the faster diffusion rate of W and C atoms in the bonding phase at higher temperature. In the same time, the increase in temperature accelerates the dissolution rate of WC particles, which contributes to the slower recrystallization and favours gradual increase of the WC grain

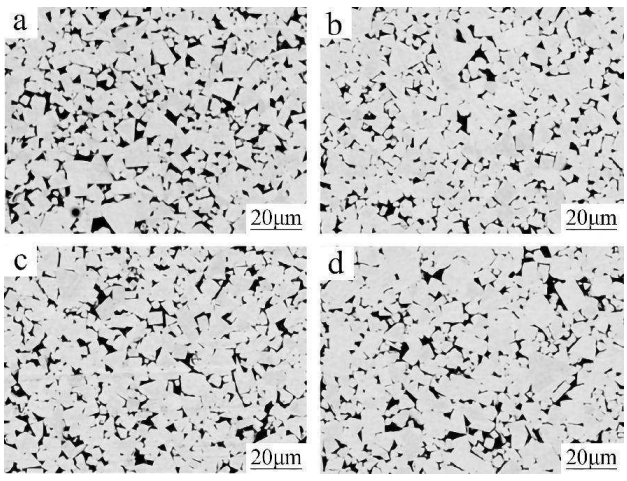

Figure 3. SEM micrographs of sintered ceramics: a) A2, b) A2, c) A3 and d) A4

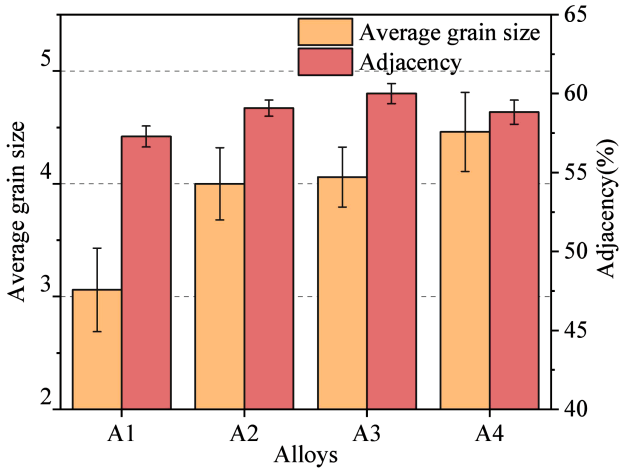

Figure 4. Average grain size vs. adjacency curve of A1-A4 ceramics

size. The recrystallization of WC grains occurs simultaneously with grain growth, and the recrystallization rate is higher than the grain growth rate when the temperature is lower, so the average grain size of WC is smaller. When the temperature gradually increases, the grain growth rate is gradually higher than the recrystallization rate, and the average grain size in the ceramics gradually increases, and this trend is consistent with data presented in Fig. 4.

Figure 5 depicts the grain size distribution of the ceramics sintered at different temperatures. It can be seen that small amount of large WC grains (≤10 μm) exists in all WC-Ni-Co ceramics, but the frequency distribution of ultra-coarse crystals >10 μm shows a decreasing and then increasing trend with the increase of the sintering temperature. This is because when the sintering temperature is 1390 °C, it is difficult to completely dissolve WC particles at lower sintering temperatures and there are more WC particles in the liquid phase, so it is easier for the residual grains to grow into ultra-coarse crystals when cooling down. When the sintering temperature increases to 1410 °C, the solubility of the bonding phase in the ceramics relative to WC phase increases,

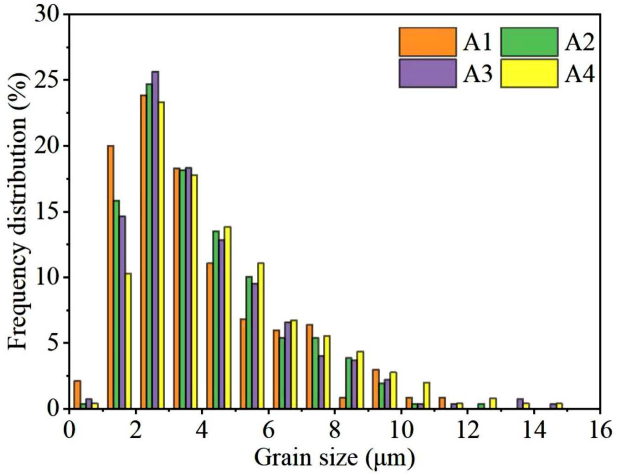

Figure 5. Grain size distribution of A1-A4 ceramics

the WC phase dissolved in the bonding phase can reach saturation and the frequency of ultra-coarse crystals in the distribution of grains is gradually reduced. However, the continued increase in sintering temperature leads to a faster dissolution rate, the recrystallization of WC grains in the liquid phase and grain growth time are prolonged, and thus the frequency of ultra-coarse crystals shows a rising trend again. When the sintering temperature is in the range of 1410–1430 °C, the difference between the average grain size and the adjacency in the microstructure of the ceramics is smaller, indicating the optimal sintering temperatures.

Densities and average grain sizes of the ceramics sintered at different temperatures are given in Table 2. With the increase of sintering temperature, density of the ceramics shows a tendency of increasing and then decreasing. The sintering temperature, as the most critical factor affecting the densification of ceramics, mainly relies on liquid-phase flow and particle rearrangement in liquid-phase sintering to improve the densification of the ceramics. When the sintering temperature is 1390 °C, the low sintering temperature leads to the slow flow rate of the liquid phase and the existence of tiny pores in the ceramics, which results in the low densification of the ceramics. As the sintering temperature continues to increase, the capillary force formed by the liquid phase and the viscous flow of the liquid phase itself can promote the movement of WC grains to achieve the tightest arrangement, and the densification of the sintered specimens gradually increases. However, when the sintering temperature is ≥1450 °C, the coarsening of the grains hinders the gas discharge, which reduces the driving force of the liquid-phase binder migration to fill the pores, leading to the decrease in the degree of densification of the ceramics, which is similar to the change rule of the sintering properties of tungsten-cobalt ceramics studied by Lisovsky [20] and Hu *et al.* [21].

Table 2. Average grain size and density of ceramics sintered at different temperatures

Sample	Grain size [μm]	Density [g/cm^3]	Relative density [%TD]
A1	3.06	14.287	98.43
A2	4.00	14.462	99.67
A3	4.05	14.488	99.86
A4	4.46	14.419	99.39

Mechanical properties

The influence of the sintering temperature on the mechanical properties of the obtained ceramics is shown in Fig. 6. The hardness and flexural strength of the ceramics both show a trend of increasing and then decreasing with the increase of sintering temperature. After the powder sintering process, densification and grain size act as decisive factors affecting the hardness of the sintered specimens and the densification contributes to the increase of hardness, while the growth of WC grains re-

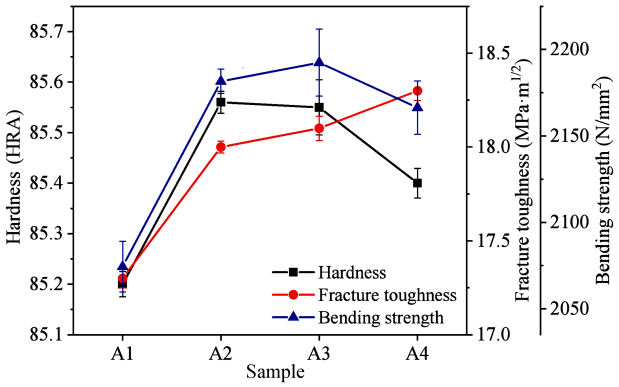

Figure 6. Influence of sintering temperature on hardness, fracture toughness and flexural strength

duces the hardness of the ceramics. When the sintering temperature is 1390 °C, the effect of densification on the ceramics properties is higher than that of grain growth and other factors, and the lower densification weakens the ability of the specimens to resist damage, resulting in the hardness, fracture toughness and flexural strength of the A1 ceramics being at a lower level. When the sintering temperature increases from 1410 to 1450 °C, the relative density of the ceramics reaches 99.5%, and there is limited space for the improvement of densification, and the mechanical properties of the ceramics are more correlated with grain growth [11,22]. Therefore, the hardness of the ceramics gradually decreases and the fracture toughness gradually increases with the increase of WC grain size.

The change of flexural strength with sintering temperature can also be observed in Fig. 6. The flexural strength of the ceramics increases and then decreases with the increase of sintering temperature, and the flexural strength of the A3 ceramics is the highest at 2192 N/mm^2. When the sintering temperature was 1390 °C, the lower densification seriously weakened the flexural strength of the ceramics, and the flexural strength of the A1 specimen was the lowest. When the sintering temperature increased from 1390 to 1410 °C, the densification of the ceramics increased the energy barrier of the fracture process in the specimen, and the flexural strength of the ceramics showed an upward trend. When the sintering temperature continued to increase, the effect of densification gradually weakened and the WC grain size became the main factor affecting the flexural strength. However, the degree of change in WC grain size between the A2 and A3 ceramics is small, and the difference in the flexural strength of ceramics is not high. When the sintering temperature rises to 1450 °C, the frequency of ultra-coarse crystals in the A3-A4 ceramics gradually increases, which significantly increases the number of fracture sources in the ceramics, and therefore the flexural strength of the ceramics tends to decrease.

SEM images of the ceramic fracture of the A1-A4 samples are shown in Fig. 7. The presence of microcracks in individual WC grains was found in the fractured A1 ceramics (Fig. 7), which was attributed to the slow shrinkage during sintering of the ceramics, resulting in relatively poor densification and therefore a weaker skeleton strength of the ceramics, which resulted in a decrease in the flexural strength. In the A2-A3 specimens, there are more fine WC grains, which can effectively reduce the number of fracture sources and impede the crack extension, and the number of perforated fractures in the fracture morphology increases gradually. The energy consumed in crack extension increases gradually and thus the flexural strength increases gradually. However, the further increase of sintering temperature reduces the critical stress for fracture of the ceramics, so the flexural strength of the A4 specimen is lower than that of the A3 specimen.

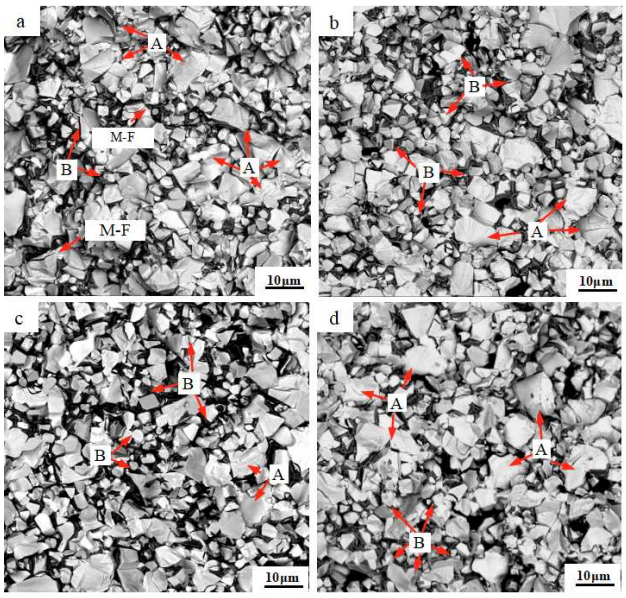

Figure 7. SEM images of fractured ceramics: a) A1, b) A2, c) A3 and d) A4 (A - fracture through crystal, B - fracture along crystal, M-F - micro-cracking)

3.2. Comparison of WC-Ni-Co and WC-Co ceramics

In order to ensure that the prepared WC-Ni-Co coarse grain ceramics meets the requirements for the use in harsh environments, two additional samples (WC-Ni-Co and WC-Co, labelled as D1 and D2, respectively) with the same WC grain size were prepared from the ultra-coarse WC starting powder and sintered at 1430 °C and argon pressure of 5 MPa. The performance of two ceramics were explored by the analysing the microstructure and mechanical properties.

Structural characterization

XRD results (Fig. 8) confirm that only two phases, hard phase WC and bonded phase (γ-(Co-Ni) phase or γ-Co phase), exist in the two ceramics. Diffraction peaks of graphite and η decarburisation phases, which are unfavourable for the ceramic properties, are not detected. Meanwhile, the peak intensity and peak width of the three strong peaks ((001), (100) and (101)) of the WC phase in the two specimens do not differ much, in-

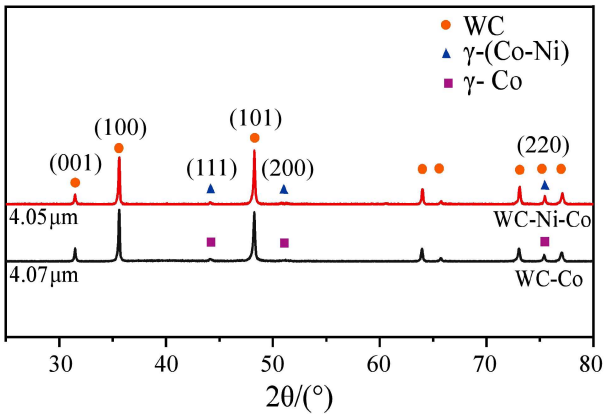

Figure 8. XRD patterns of WC-Ni-Co and WC-Co ceramics

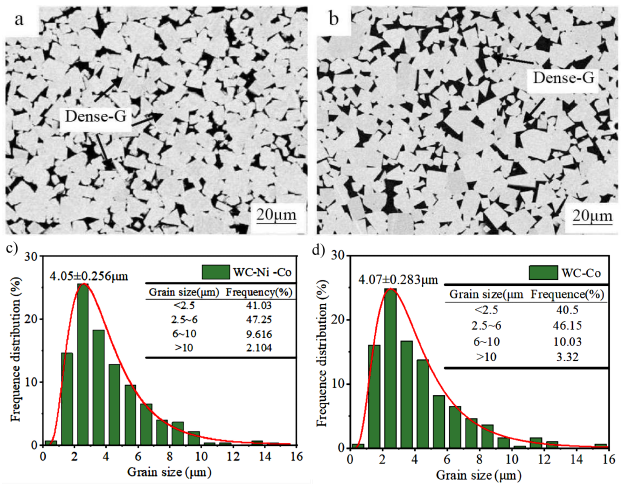

Figure 9. SEM images of: a) WC-Ni-Co and b) WC-Co ceramics, as well as grain distribution curves of: c) WC-Ni-Co and d) WC-Co ceramics

dicating that the WC crystallinity of the WC-Ni-Co and WC-Co specimens are basically the same, which is in agreement with the microscopy images of the ceramics in Fig. 9a,b.

SEM image analysis of the D1 and D2 specimens are shown in Fig. 9a,b. The dark area indicates the metallic bonding phase. It can be seen that there is not much difference in the average grain size between two ceramics, but it seems that size distribution of the D1 ceramics is narrower (Fig. 9c,d).

It is also interesting to underline that the WC-Ni-Co ceramics prepared from the ultra-coarse WC powder (specimen D1) and the mixture of ultra-coarse and fine WC particles (sample A3) have the same average grain size (Table 2 and Fig. 9c). However, it seems that the frequency of WC grains <2.5 μm in the A3 specimen is higher and the frequency of ultra-coarse crystals >10 μm is lower than that of the D1 specimen. This is because the addition of the fine-grained WC facilitates the flow of the liquid phase and the fine WC particles can easily migrate to the middle of the coarse-grained WC during the liquid-phase sintering stage, and the gradual growth of the WC grains during the cooling down leads to the decrease of the mean free range of the ceramics and the significant increase of the degree of adjacency. The mean free range is the average distance passed by a grain colliding with other grains [15].

Mechanical properties

The difference in density as well as the difference in hardness, fracture toughness and flexural strength (Table 3) between the two ceramics is relatively small, but some fluctuations still exist. This is because the WC grain size and ultra-coarse grain frequency distribution of the two ceramics do not differ much, but the WC grains in the WC-Ni-Co coarse-crystalline ceramics are arranged more closely, and the specimen can show higher surface strength when pressed, so the hardness of the WC-Ni-Co ceramics is on the high side. At the same time, the fracture toughness is low due to the high degree of adjacency in the WC-Ni-Co ceramics, which results in low energy consumption during the crack expansion. The difference in flexural strength can be explained by the theory of grain distribution. When ceramics contain two types of WC grains, fine grains will exist between the coarse grains, which is favourable for reducing the energy required for crack expansion. The WC-Ni-Co ceramics is compressed when the crack expansion rate is faster, and the WC-Co ceramics with higher frequency of the ultra-coarse grains has higher number of fracture sources, which accelerates the aggregation of the micro-cracks. Thus, the difference in flexural strength between the two ceramics is very small. Quantitative analysis of the above data, the hardness, fracture toughness and flexural strength, between the two ceramics shows that the difference is within 1%, so the mechanical properties of the two ceramics are basically the same.

Wear resistance analysis

Wear resistance curves of the prepared ceramics (Fig. 10) indicate that there is a difference of 0.03 mg (about 10%) between the mass loss of the WC-Ni-Co and WC-Co specimens in the reciprocating friction wear experiment. The wear-resistant coefficients of the two specimens after the test of the steel wheel method are also basically the same. Thus, two measurements show that there is not much difference in wear-resistant properties between the obtained ceramics. In addition, the ceramics wear resistance coefficient first increases steeply and

Table 3. Comparative analysis of the mechanical properties of ceramics

No.	Components	Grain size [μm]	Density [g/cm^3]	Durometer [HRA]	Fracture toughness [MPa·m$^{1/2}$]	Bending strength [N/mm^2]
D1	WC-Ni-Co	4.05	14.49	85.61	18.17	2190
D2	WC-Co	4.07	14.43	85.58	18.20	2210

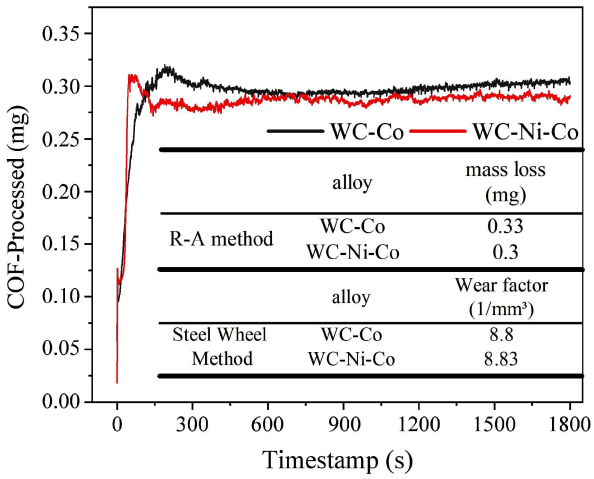

Figure 10. Graph of wear resistance coefficient of ceramics

then enter the stable wear stage around 300 s. It can also be seen from the stable wear stage of the two ceramics that the wear resistance curve of the WC-Ni-Co ceramics is lower than that of the WC-Co ceramics, but the curve fluctuation trend is larger. This is due to the phenomenon of unstable wear of the ceramics caused by the shedding of WC particles with the prolongation of wear time.

In order to facilitate further insight in the wear mechanism, SEM analysis of the wear ceramic surfaces was performed (Fig. 11). It can be seen that the number of fine and medium-coarse WC grains in the WC-Ni-Co ceramics is relatively large. The fine WC grains in the ceramics can impede the abrasive wear, and the presence of medium-coarse WC particles can ensure the stability of the bonding phase. The finer WC grains are not easy to break during wear, which contribute to the improvement of the surface strength of the specimen. Higher amount of the ultra-coarse crystals, which easily break during wear in the WC-Co ceramics leads to the rise of the number of micro-abrasive grains on the ceramic surface. It can also be seen from Fig. 11a that the increase in the frequency of fine grains leads to more WC grain shedding in the wear surface of the D1 ceramics. However, more ultra-coarse grains in the D2 ceramics are easily broken, leading to an increase in the number of surface micro-abrasive grains (Fig. 11b). Under the combined effect of these two, the wear resistance of the WC-Ni-Co and WC-Co ceramics is not much different.

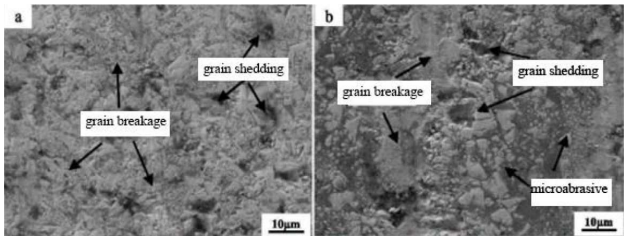

Figure 11. SEM images of the wear ceramic surfaces of: a) WC-Ni-Co and b) WC-Co ceramics

The elemental analysis of the wear surface of the ceramics (not shown here) confirmed that most of the residual Co bonding phase in the WC-Co ceramics exists in the grain crushing region, which indicates that the ultra-coarse grains are crushed first during the wear and increase the degree of surface deterioration of the ceramics. Co and Ni are mostly present around the WC grains indicating that the wear of the bonded phase leads to the detachment of WC grains. The shedding of grains leads to large fluctuations in the wear resistance curve. However, higher amount of the ultra-coarse crystals, which easily break during wear, in the WC-Co leads to the rise of the number of micro-abrasive grains on the ceramic surface.

Corrosion resistance

Figure 12 shows the variation curves of corrosion rate of D1 and D2 ceramics in NaCl solution. The Tafel curve graph (Fig. 12) and Table 4 confirm that the self-corrosion potential is higher and the self-corrosion current density is lower for the WC-Ni-Co. The self-corrosion potential indicates the corrosion tendency of ceramics and the self-corrosion current indicates the corrosion rate of ceramics. From the kinetic point of view, the corrosion rate and corrosion tendency of the WC-Co ceramics are larger and the corrosion resistance of the WC-Ni-Co ceramics is better.

By comparing the Tafel curves of the two ceramics, it can be seen that both WC-Co and WC-Ni-Co ceramics show different degrees of passivation during the corro-

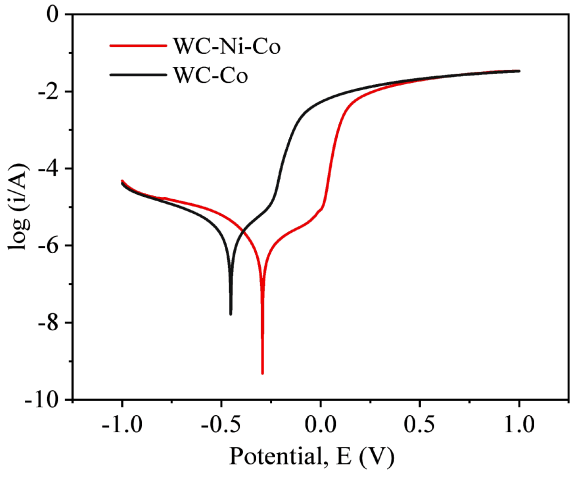

Figure 12. Electrochemical polarisation curves of ceramics in NaCl solution

Table 4. Electrochemical corrosion parameters of ceramics in NaCl solution

Sample	E_{corr} [V]	I_{corr} [A/cm^2]	Mean free range [μm]	Adjacency [%]
D1	−0.293	7.887×10^{-7}	1.4021	60.2
D2	−0.453	1.62×10^{-6}	2.166	50.28

sion process, but WC-Co ceramics has a higher breakdown current density. This is because the thermodynamic stability of Co in the passivation zone is lower than that of Ni. It can also be shown from the thermodynamic point of view that the WC-Ni-Co ceramics has better corrosion resistance than WC-Co ceramics.

Figure 13 shows the microscopic morphology of the electrochemically corroded surfaces of the ceramic specimens. It can be observed that the binder phase on the surface layer of both ceramic specimens was corroded, but the grain morphology of WC in the corrosion pit of the WC-Co ceramics (Fig. 13b) can be clearly observed, while the grain morphology in the corrosion pit of the WC-Ni-Co ceramics (Fig. 13a) is not obvious, and there still exists a part of the non-corroded binder phase. It has been pointed out [23,24] that the corrosion mechanism of ceramics in NaCl solution is the diffusion corrosion from the core part of the bonded phase to the surrounding. Thus, the lower mean free range can reduce the contact area of WC grains with the bonded phase, and reduce the corrosion rate of the bonded phase per unit time. In addition, higher degree of adjacency can cut off the connection between the surface layer and the internal bonding phase, and increase the residual amount of the internal bonding phase in the ceramics. Our results show that the WC-Ni-Co ceramics has a higher degree of adjacency and lower average free range, thus the corrosion rate of the WC-Ni-Co ceramics bonded phase in the neutral medium might be lower and from the perspective of the corrosion mechanism the WC-Ni-Co ceramics corrosion resistance could be better.

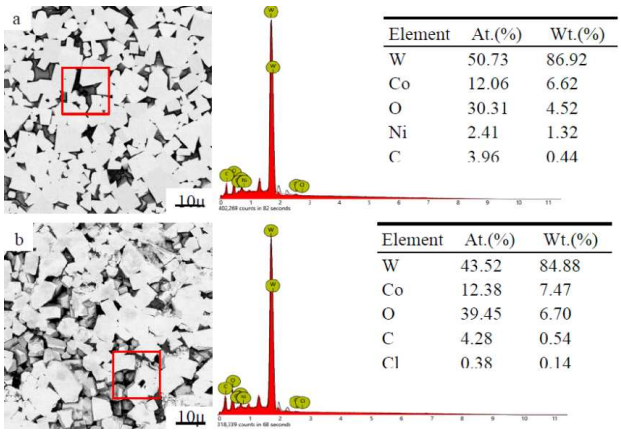

Figure 13. Micro-morphology and energy spectrum analysis of ceramics after corrosion in NaCl solution: a) WC-Ni-Co ceramics and b) WC-Co ceramics

From Fig. 13, it can be seen that there are a large number of WC grains exposed on the surface after the ceramics is corroded, and the surface becomes relatively loose. From that it can be presumed that the corrosion in NaCl solution is mainly performed on the metallic bonding phase and corresponding reaction formulas in NaCl solution are: $Ni \rightarrow Ni^{2+} + 2\,e^{-}$ and $Co \rightarrow Co^{2+} + 2\,e^{-}$.

Through the EDS analysis of the corroded surface of the ceramics, it can be seen that the residual amount of Co and Ni elements in the bonding phase of the WC-Ni-Co specimen after electrochemical corrosion is 7.94%, which is higher than the content of Co element in the bonding phase of the WC-Co specimen. This indicates that the corrosion rate of Ni in ceramics is much smaller than that of Co, and the addition of some Ni in ceramics can suppress the corrosion rate of the bonded phase. In summary, WC-Ni-Co ceramics has better corrosion resistance than WC-Co ceramics in neutral medium.

When selecting the shield cutting tool material by the grain size, hardness and fracture toughness with the same grain size of the WC-Ni-Co and WC-Co ceramics, it is obvious that the mechanical properties are not much different, but the WC-Ni-Co ceramics shows higher corrosion resistance. Thus, the comprehensive performance of the WC-Ni-Co coarse-grained ceramics is better than that of the WC-Co ceramics with the same grain size and the use of the WC-Ni-Co ceramics as a shield cutting tool material can satisfy the conditions of use in harsh environments.

IV. Conclusions

The effect of sintering temperature on the microstructure and mechanical properties of WC-Ni-Co coarse grain ceramics was analysed. In addition, the reasons and mechanisms for the differences in microstructure and mechanical properties between WC-Co ceramics and WC-Ni-Co ceramics with the same WC grain size were further analysed, and the main conclusions are as follows:

1. WC-Ni-Co rough crystalline ceramics was generated by sintering at different temperatures between 1390 and 1450 °C. With the increase of sintering temperature the frequency of ultra-coarse grains in the microstructure of the ceramics showed a trend of first increasing and then decreasing, and the average grain size gradually increased with the increase of sintering temperature.
2. When the sintering temperature is 1390 °C, the density of the ceramics is low, and the residual porosity in the ceramics results in low hardness, fracture toughness and flexural strength. With the increase in temperature, the increase in densification promotes the improvement of the mechanical properties of the ceramics. However, when the sintering temperature is between 1410 and 1430 °C, the relative density is the highest and the average grain size is the main factor affecting the mechanical properties. Therefore, when the sintering temperature rises to 1450 °C, the frequency of ultra-coarse crystals in the microstructure increases rapidly, resulting in a gradual decrease in hardness and flexural strength. The best properties of the ceramics were obtained when the sintering temperature was 1410 and 1430 °C.
3. WC-Co ceramics with the same grain size as WC-Ni-Co ceramics was prepared by using ultra-coarse

grains under the same experimental conditions. SEM analysis, XRD physical phase analysis and grain distribution studies show that the two ceramics do not differ much in grain size, and there are no decarburisation and graphite and other impurity phases within the ceramics.

4. When the average grain size is the same, the difference between the densities of WC-Ni-Co and WC-Co ceramics is very small, and the properties of the ceramics, such as the hardness, fracture toughness and flexural strength, are all within 1% difference. However, the WC-Ni-Co ceramics exhibits similar abrasion resistance but higher corrosion resistance in comparison to the WC-Co ceramics. Therefore, WC-Ni-Co ceramics, which adopts ultra-coarse WC particles paired with fine-grained WC to solve the phenomenon of grain coarsening, can be used instead of WC-Co ceramics as shield cutting tool material.

Acknowledgements: This study was supported by Natural Science Foundation of Shandong Province (ZR2021ME182), State Key Laboratory of Material Forming and Mould Technology Open Fund Project(P12), National Natural Science Foundation of China (52001187), the Science and Technology Enterprise Innovation Program of Shandong Province, China (2023TSGC085, 2023TSGC0119, 2023TSGC0759 and 2023TSGC0961) and Shandong Province Development and Reform Commission Special Needs Talents Project: R&D and Application of Intelligent Manufacturing Key Technology for High Performance Railway Wheel Unit Production Line (JNGC2023001)

References

1. J. Garcia, V.C. Cipres, A. Blomqvist, B.Kaplan, "Cemented carbide microstructures: A review", *Int. J. Refract. Met. Hard Mater.*, **80** (2019) 40–68.
2. G.S. Upadhyaya, "Materials science of cemented carbides - An overview", *Mater. Des.*, **22** [6] (2001) 483–489.
3. F. Lofaj, Y.S. Kaganovskii, "Kinetics of WC-Co oxidation accompanied by swelling", *J. Mater. Sci.*, **30** [7] (1995) 1811–1817.
4. X. Ren, H. Zou, Q. Diao, C. Wang, Y. Wang, H. Li, T. Sui, B. Lin, S.Yan, "Surface modification technologies for enhancing the tribological properties of cemented carbides: A review", *Tribol. Int.*, **180** (2023) 108257.
5. D.K. Shetty, I.G. Wright, P.N. Mincer, A.H. Clauer, "Indentation fracture of WC-Co cermets", *J. Mater. Sci.*, **20** [5] (1985) 1873–1882.
6. A. Bose, J.P. Reidy, J. Pötschke, "Sinter-based additive manufacturing of hardmetals: Review", *Int. J. Refract. Met. Hard Mater.*, **119** (2024) 106493.
7. I. Konyashin, B. Ries, *Cemented Carbides*, Burghaun, Germany, 2022.
8. C. Chen, B.Y. Huang, Z.M. Liu, Y.X. Li, D. Zou, T. Liu, Y.M. Chang, L. Chen, "Additive manufacturing of WC-Co cemented carbides: Process, microstructure, andmechanical properties", *Addit. Manufact.*, **63** [5] (2023) 103410.
9. Y.C. Wu, Z.Y. Lu, Y.Q. Qin, Z.Y. Boa, L.M. Lou, "Ultrafine/nano WC-Co cemented carbide: Overview of preparation and key technologies", *J. Mater. Res. Technol.*, **27** (2023) 5822–5839.
10. W. Su, Yx. Sun, J. Liu, F. Jiao, J.M. Ruan, "Effects of Ni on the microstructures and properties of WC-6Co cemented carbides fabricated by WC-6(Co,Ni) composite powders", *Ceram. Int.*, **41** [2] (2015) 3169–3177.
11. C. Bertalan, S. Moseley, L. Pereira, R. Useldinger, "Influence of sintering parameters on the microstructure and mechanical properties of WC-Co hardmetals", *Int. J. Refract. Met. Hard Mater.*, **118** (2024) 106439.
12. D.D. Phuong, P.V. Trinh, L.V. Duong, L.D. Chung, "Influence of sintering temperature on microstructure and mechanical properties of WC-8Ni cemented carbide produced by vacuum sintering", *Ceram. Int.*, **42** [13] (2016) 14937–14943.
13. G.L. Zhu, J.C. Peng, W.Y. Li, Q. Wang, "Research on vacuum sintering and low-pressure sintering of cemented carbide", *Tool Technol.*, **49** [7] (2015) 31–33.
14. R.C. Desia, R. Kapral, "Lifshitz-Slyozov-Wagner theory", pp. 87–95 in *Dynamics of Self-Organized and Self-Assembled Structures*, Cambridge University Press, 2009.
15. Z. Roulon, J.M. Missiaen, S. Lay, "Carbide grain growth in cemented carbides sintered with alternative binders", *Int. J. Refract. Met. Hard Mater.*, **86** (2020) 105088.
16. S. Yang, J.B. Gu, J. Liao, H.X. Chen, "Effect of sintering pressure on the organization and properties of WC-12%Co rough crystal cemented carbide", *Rare Met. Cemented Carbides*, **50** [2] (2015) 54–58.
17. M. Li, X.F. Gan, H.G. Zhang, "Effect of carbon content on the microstructure and properties of WC-5.7%Co-5.7%Ni-0.13%Cr cemented carbide", *Rare Met. Cemented Carbides*, **50** [3] (2015) 87–92.
18. A.S. Kurlov, A.I. Gusev, *Tungsten Carbides: Structure, Properties and Application in Hardmetals*, Springer International Publishing, Russia, 2013.
19. M.L. He, X.Y. Zheng, H.X. Tian, H. Mao, Y. Du, "Residual thermal stress, fracture toughness, and hardness in WC-Co cemented carbides: Finite element simulation and experimental verification", *J. Mater. Res. Technol.*, **21** (2022) 2445–2454.
20. A.F. Lisovsky, "The thermodynamics of the liquid phase migration in nanodispersed composite bodies", *Int. J. Heat Mass Transfer*, **52** (2009) 4766–4768.
21. H.P. Hu, Y. Cheng, Z.B. Yin, Y.Zhang, T.Y. Lu, "Mechanical properties and microstructure of Ti(C, N) based cermet cutting tool materials fabricated by microwave sintering", *Ceram. Int.*, **41** (2015) 15017–15023.
22. X. Wang, D. Zhou, P. Xu, "The WC-Co/Fe-Ni interface: Effect of holding time on the microstructure, grain size and grain growth mechanism", *Ceram. Int.*, **45** [17] (2019) 23320–23327.
23. B. Han, W. Dong, B.W. Fan, S.G.Zhu, "Comparison on the immersion corrosion and electrochemical corrosion resistance of WC-Al_2O_3 composites and WC-Co cemented carbide in NaCl solution", *RSC Advances*, **11** [36] (2021) 22495–22507.
24. A.M. Human, H.E. Exner, "Electrochemical behaviour of tungsten-carbide hardmetals", *Mater. Sci. Eng.*, **209** [1–2] (1996) 180–191.